ORIGINAL RESEARCH • NEURORADIOLOGY

Radiology

Brain MRI Findings in Severe COVID-19: A Retrospective Observational Study

*Stéphane Kremer, MD, PhD** • *François Lersy, MD** • *Jérome de Sèze, MD, PhD* • *Jean-Christophe Ferré, MD, PhD* • *Adel Maamar, MD* • *Béatrice Carsin-Nicol, MD* • *Olivier Collange, MD, PhD* • *Fabrice Bonneville, MD, PhD* • *Gilles Adam, MD* • *Guillaume Martin-Blondel, MD, PhD* • *Marie Rafiq, MD* • *Thomas Geeraerts, MD, PhD* • *Louis Delamarre, MD* • *Sylvie Grand, MD* • *Alexandre Krainik, MD, PhD* • *For the SFNR-COVID Group*[1]

From the Hôpitaux Universitaires de Strasbourg, Service d'Imagerie 2, Hôpital de Hautepierre, Strasbourg, France (S.K.). Received May 15, 2020; revision requested May 21; revision received June 8; accepted June 19. **Address correspondence to** S.K. (e-mail: *stephane.kremer@chru-strasbourg.fr*).

[1] The complete list of authors and affiliations is at the end of this article.

*S.K. and F.L. contributed equally to this work.

Radiology 2020; 297:E242–E251 • https://doi.org/10.1148/radiol.202020222 • Content code: NR

Background: Brain MRI parenchymal signal abnormalities have been associated with severe acute respiratory syndrome coronavirus 2 (SARS-CoV-2).

Purpose: To describe the neuroimaging findings (excluding ischemic infarcts) in patients with severe coronavirus disease 2019 (COVID-19) infection.

Materials and Methods: This was a retrospective study of patients evaluated from March 23, 2020, to April 27, 2020, at 16 hospitals. Inclusion criteria were (*a*) positive nasopharyngeal or lower respiratory tract reverse transcriptase polymerase chain reaction assays, (*b*) severe COVID-19 infection defined as a requirement for hospitalization and oxygen therapy, (*c*) neurologic manifestations, and (*d*) abnormal brain MRI findings. Exclusion criteria were patients with missing or noncontributory data regarding brain MRI or brain MRI showing ischemic infarcts, cerebral venous thrombosis, or chronic lesions unrelated to the current event. Categorical data were compared using the Fisher exact test. Quantitative data were compared using the Student *t* test or Wilcoxon test. $P < .05$ represented a significant difference.

Results: Thirty men (81%) and seven women (19%) met the inclusion criteria, with a mean age of 61 years ± 12 (standard deviation) (age range, 8–78 years). The most common neurologic manifestations were alteration of consciousness (27 of 37, 73%), abnormal wakefulness when sedation was stopped (15 of 37, 41%), confusion (12 of 37, 32%), and agitation (seven of 37, 19%). The most frequent MRI findings were signal abnormalities located in the medial temporal lobe in 16 of 37 patients (43%; 95% confidence interval [CI]: 27%, 59%), nonconfluent multifocal white matter hyperintense lesions seen with fluid-attenuated inversion recovery and diffusion-weighted sequences with variable enhancement, with associated hemorrhagic lesions in 11 of 37 patients (30%; 95% CI: 15%, 45%), and extensive and isolated white matter microhemorrhages in nine of 37 patients (24%; 95% CI: 10%, 38%). A majority of patients (20 of 37, 54%) had intracerebral hemorrhagic lesions with a more severe clinical presentation and a higher admission rate in intensive care units (20 of 20 patients [100%] vs 12 of 17 patients without hemorrhage [71%], $P = .01$) and development of the acute respiratory distress syndrome (20 of 20 patients [100%] vs 11 of 17 patients [65%], $P = .005$). Only one patient had SARS-CoV-2 RNA in the cerebrospinal fluid.

Conclusion: Patients with severe coronavirus disease 2019 and without ischemic infarcts had a wide range of neurologic manifestations that were associated with abnormal brain MRI scans. Eight distinctive neuroradiologic patterns were described.

Severe acute respiratory syndrome coronavirus 2 (SARS-CoV-2) is the seventh member of the family of coronaviruses that infect humans (1) and induces coronavirus disease 2019 (COVID-19). Human coronaviruses have neuroinvasive capacities and may be neurovirulent by two main mechanisms (2–4): viral replication into glial or neuronal cells of the brain or autoimmune reaction with a misdirected host immune response (5). Thus, a few cases of acute encephalitislike syndromes with human coronaviruses were reported in the past 2 decades (5–8). In regard to COVID-19, current data on central nervous system involvement are uncommon but growing (9–17), demonstrating the high frequency of neurologic symptoms.

However, the delineation of a large cohort of confirmed brain MRI parenchymal signal abnormalities (excluding ischemic infarcts) related to COVID-19 has never been performed, and the underlying pathophysiologic mechanisms remain unknown. The purpose of the current study was to describe the neuroimaging findings (excluding ischemic infarcts) in patients with severe COVID-19 and report the clinicobiologic profile of these patients.

Materials and Methods

This retrospective observational national multicenter study was initiated by the French Society of Neuroradiology in collaboration with neurologists, intensivists, and infectious disease specialists and brought together 16 hospitals. The study was approved by the ethical committee of Strasbourg University Hospital (CE-2020–37) and was in accordance with the 1964 Helsinki Declaration and its later amendments. Because of the emergency in the context of the COVID-19 pandemic responsible for

Abbreviations

COVID-19 = coronavirus disease 2019, FLAIR = fluid-attenuated inversion recovery, SARS-CoV-2 = severe acute respiratory syndrome coronavirus 2, WM = white matter

Summary

Eight distinctive neuroradiologic patterns (excluding ischemic infarcts) were identified in patients with severe coronavirus disease 2019 infection and abnormal brain MRI findings.

Key Results

- In patients with coronavirus disease 2019 (COVID-19), the most frequent neuroimaging features were involvement of the medial temporal lobe, nonconfluent multifocal white matter (WM) hyperintense lesions on fluid-attenuated inversion recovery images with variable enhancement and hemorrhagic lesions, and extensive and isolated WM microhemorrhages.
- Most of the patients in this study had intracerebral hemorrhagic lesions, which were associated with worse clinical status.
- Of 37 patients, only one had positive findings for severe acute respiratory syndrome coronavirus 2 in the cerebrospinal fluid.

acute respiratory and neurologic manifestations, the requirement for patient written informed consent was waived.

Patient Cohort

Consecutive patients with COVID-19 infection and neurologic manifestations who underwent brain MRI were included from March 23, 2020, to April 27, 2020, in 16 French centers, including 11 university hospitals and five general hospitals. Inclusion criteria were (*a*) diagnosis of COVID-19 based on possible exposure history or symptoms that were clinically compatible with the disease, validated with detection of SARS-CoV-2 via reverse transcriptase polymerase chain reaction assays on the nasopharyngeal, throat, or lower respiratory tract swabs; (*b*) severe COVID-19 infection defined as requirement for hospitalization and oxygen therapy; (*c*) neurologic manifestations; and (*d*) abnormal brain MRI with acute or subacute abnormalities. Exclusion criteria were (*a*) patients with missing or noncontributory data (lack of sequences, numerous artifacts) regarding brain MRI or (*b*) brain MRI showing ischemic infarcts, cerebral venous thrombosis, or chronic lesions unrelated to the current event.

Clinical and laboratory data were extracted from the patients' electronic medical records in the hospital information system. Only laboratory analyses within 3 days before brain MRI were considered. In the case of redundancy of the tests, the worst value was kept. Clinical and biologic data were reviewed by two neurologists (J.D.S., M.A.; 25 and 15 years of clinical expertise in neurology, respectively) and one virologist (S.F.K). They participated in elaboration of the study design, interpretation of the data, and manuscript editing. When available, all electroencephalograms were reviewed by one expert neurologist (C.B., 30 years of experience) and classified into five groups (normal, under sedation, nonspecific, encephalopathy, or seizures).

Virologic Assessment

Quantitative real-time reverse transcriptase polymerase chain reaction tests for SARS-CoV-2 nucleic acid were performed on nasopharyngeal or lower respiratory tract swabs as well as cerebrospinal fluid. Primer and probe sequences target two regions on the RNA-dependent RNA polymerase (RdRp) gene and are specific to SARS-CoV-2. Assay sensitivity is around 10 copies per reaction (in-house method, Institut Pasteur, Paris, France) (18).

Brain MRI Protocols

Imaging studies were conducted on either a 1.5- or 3.0-T MRI machine. The multicenter nature of the study and the various clinical setups did not allow standardization of sequences. The most frequently performed sequences were three-dimensional T1-weighted spin-echo MRI with or without contrast enhancement, diffusion-weighted imaging, gradient-echo T2- or susceptibility-weighted imaging, and two- or three-dimensional fluid-attenuated inversion recovery (FLAIR) imaging after administration of a gadolinium-based contrast agent.

MRI Interpretation

After anonymization, images were presented to readers on a picture archiving and communication system (General Electric, Milwaukee, Wis). After review of MRI studies by three neuroradiologists (S.K., F.C., F.L.; 20, 25, and 9 years of experience in neuroradiology, respectively) who were blinded to all patient data, brain MRI findings were divided by consensus into eight groups: (*a*) unilateral hyperintensities located in the medial temporal lobe on FLAIR or diffusion-weighted images; (*b*) an ovoid hyperintense lesion located in the central part of the splenium of the corpus callosum on FLAIR and diffusion-weighted images; (*c*) nonconfluent multifocal white matter (WM) hyperintense lesions with variable enhancement on FLAIR and diffusion-weighted images; (*d*) nonconfluent multifocal WM hyperintense lesions with variable enhancement associated with hemorrhagic lesions on FLAIR and diffusion-weighted images; (*e*) acute necrotizing encephalopathy (9) when symmetric thalamic lesions (edema, petechial hemorrhage, and necrosis), with variable involvement of the brainstem, internal capsule, putamen, cerebral, and cerebellar WM; (*f*) extensive and isolated WM microhemorrhages; (*g*) extensive and confluent supratentorial WM hyperintensities on FLAIR images; and (*h*) hyperintense lesions involving both middle cerebellar peduncles on FLAIR images. Patients could have had more than one pattern.

Statistical Analysis

Data were described using frequency and proportion for categorical variables and using mean, median, interquartile range, and range for quantitative data. In a second step, patients with hemorrhagic lesions were gathered into one group, termed *patients with hemorrhagic complications*, to look for clinicobiologic differences between the two populations. Categorical data were compared using the Fisher exact test. Quantitative data were compared by using the Student *t* test or Wilcoxon test. $P < .05$ represented a significant difference.

Results

Between March 23, 2020, and April 27, 2020, 190 consecutive patients with COVID-19 infection and neurologic manifestations underwent brain MRI in 16 hospitals. All patients with normal brain MRI findings, ischemic infarcts, cerebral venous thrombosis, or chronic lesions unrelated to the current event were excluded. A total of 37 patients with COVID-19 infection were finally included in this study (Fig 1). The average age of the patients was 61 years ± 12 (standard deviation), with 30 men and seven women included (Table 1). Most of these patients (32 of 37, 87%) were admitted to intensive care units because of acute respiratory failure. The most frequent neurologic manifestations were alteration of consciousness (27 of 37, 73%), pathologic wakefulness after sedation (15 of 37, 41%), confusion (12 of 37, 32%), and agitation (seven of 37, 19%).

Among the 26 electroencephalograms obtained, two (8%) were considered normal, six (23%) were obtained with the patient sedated, 10 (39%) showed nonspecific findings, seven (27%) were classified as showing encephalopathy, and one (4%) revealed seizures. At the end of the study, the mortality rate was 14%. The blood counts of patients showed leukocytosis, lymphopenia, and anemia. Patients had elevated serum levels of C-reactive protein, ferritin, alanine aminotransferase, aspartate aminotransferase, urea, creatinine, fibrinogen, and D-dimers (Table 2). Fifteen of 19 patients (79%) had positive results for the presence of a lupus anticoagulant.

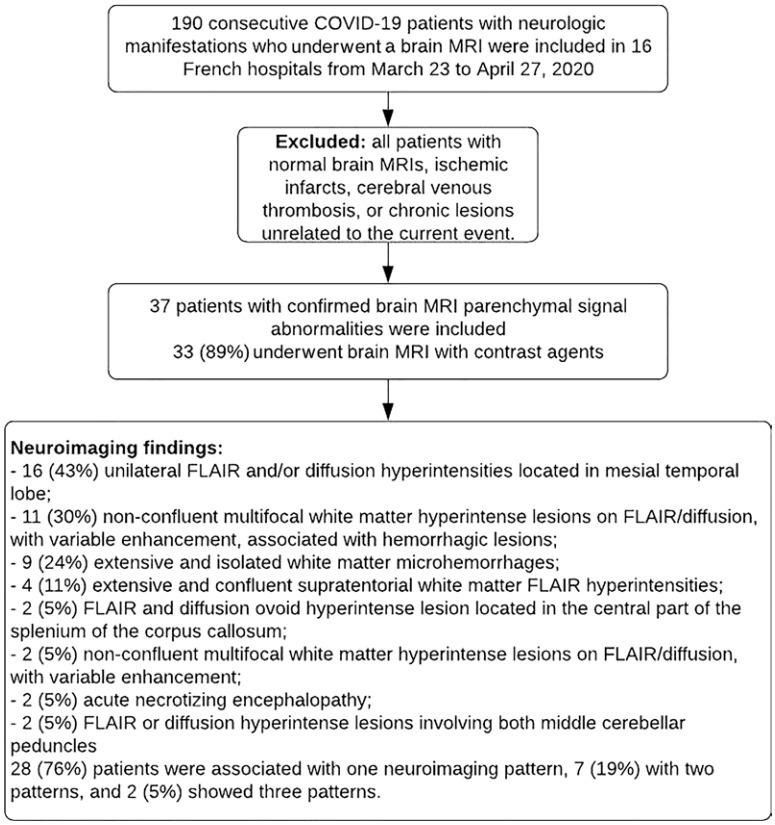

Figure 1: Flowchart shows patient inclusion and exclusion criteria. COVID-19 = coronavirus disease 2019, FLAIR = fluid-attenuated inversion recovery.

Thirty-one patients underwent a lumbar puncture, and among them, 21 (68%) had increased markers of inflammation (high white blood cell count, high proteinorachia, elevated immunoglobulin G level, or a combination thereof). One patient demonstrated the presence of SARS-CoV-2 on a reverse transcriptase polymerase chain reaction assay. High levels of interleukin-6 were found in two of six patients (Table 3).

Neuroimaging Findings

The results of MRI findings are summarized in Figure 1. Among the 37 patients included, 28 (76%) were associated with one neuroimaging pattern, seven (19%) were associated with two patterns, and two (5%) showed three patterns (Figs 1–6). The most frequent neuroimaging findings among the 37 patients included were signal abnormalities located in the medial temporal lobe in 16 patients (43%; 95% confidence interval: 27%, 59%) (Fig 2), nonconfluent multifocal WM hyperintense lesions on FLAIR and diffusion-weighted images with variable enhancement associated with hemorrhagic lesions in 11 patients (30%; 95% confidence interval: 15%, 45%) (Fig 3), and extensive and isolated WM microhemorrhages in nine patients (24%; 95% confidence interval: 10%, 38%) (Fig 4).

Comparison of Patient Groups with and without Hemorrhagic Lesions

The comparison between patients with and those without intracerebral hemorrhagic lesions shows that the hemorrhagic complications were more frequently associated with intensive care unit admission (20 of 20 [100%] vs 12 of 17 [71%], P = .01), with acute respiratory distress syndrome (20 of 20 [100%] vs 11 of 17 [65%], P = .005), and with pathologic wakefulness when sedative therapies were stopped (13 of 20 [65%] vs two of 17 [12%], P = .002). The time between onset of symptoms (most often respiratory) and brain MRI was longer in patients with intracerebral hemorrhagic lesions (mean duration, 33 days vs 19 days; $P < .001$). Leukocytosis (median of 13.4×10^9/L vs 10.4×10^9/L, P = .03), anemia (median of 87 g/L vs 110 g/L, $P < .001$), and renal dysfunction (median urea level, 18 mmol/L vs 7 mmol/L; P = .026) were more pronounced in patients with hemorrhagic lesions.

Discussion

Among the eight groups of brain MRI features classification, three main neuroradiologic patterns appeared more frequently in patients with severe coronavirus disease 2019: signal abnormalities located in the medial temporal lobe; nonconfluent multifocal white matter (WM) hyperintense lesions on fluid-attenuated inversion recovery and diffusion-weighted images with variable enhancement, associated with hemorrhagic lesions; and extensive and isolated WM

Table 1: Epidemiologic Profile and Clinical Characteristics

Demographic and Clinical Parameters	All Patients (*n* = 37)	Nonhemorrhagic Forms (*n* = 17)	Hemorrhagic Forms (*n* = 20)	*P* Value
Sex				.41
Male	30 (81)	15 (88)	15 (75)	
Female	7 (19)	2 (12)	5 (25)	
Age (y)*	61 (8–78)	58 (8–73)	64 (51–78)	.11
Time from onset of symptoms† to first hospital admission (d)* mean/median/range	7 (0–30) [7]	7 (0–15) [7]	8 (3–30) [7]	.71
Time from onset of symptoms to brain MRI (d), mean/median/range†	27 (1–46) [27]	19 (1–32) [21]	33 (21–46) [33]	<.001
Oxygen therapy	36 (97)	16 (94)	20 (100)	.45
Acute respiratory distress syndrome	31 (84)	11 (65)	20 (100)	.005
Admitted in intensive care units	32 (87)	12 (71)	20 (100)	.01
Death of the patient	5 (14)	1 (6)	4 (20)	.34
Medical history				
History of stroke	7 (19)	1 (6)	6 (30)	.09
History of seizures	1 (3)	1 (6)	0	.45
Another neurologic history	8 (22)	5 (29)	3 (15)	.42
Neurologic manifestations				
Headaches	4 (11)	3 (18)	1 (5)	.31
Seizures	5 (14)	2 (12)	3 (15)	<.99
Clinical signs of corticospinal tract involvement	4 (11)	1 (6)	3 (15)	.6
Disturbance of consciousness	27 (73)	10 (59)	17 (85)	.13
Confusion	12 (32)	8 (47)	4 (20)	.15
Agitation	7 (19)	5 (29)	2 (10)	.21
Abnormal wakefulness in intensive care units	15 (41)	2 (12)	13 (65)	.002

Note.—Unless otherwise indicated, data are numbers of patients, and data in parentheses are percentages.

* Data are means, with ranges in parentheses and medians in brackets.

† Most often respiratory.

Table 2: Laboratory Findings

Laboratory Finding	All Patients (*n* = 37)	Nonhemorrhagic Forms (*n* = 17)	Hemorrhagic Forms (*n* = 20)	*P* Value
White blood cell count ($\times 10^9$/L) (*n* = 36)	11.8 (8.2–15)	10.4 (7.6–13.7)	13.4 (10–19.2)	.03
Lymphocyte count ($\times 10^9$/L) (*n* = 36)	1.09 (0.65–1.5)	1.22 (0.52–1.47)	1.06 (0.79–1.5)	.8
Hemoglobin level (g/L) (*n* = 36)	97 (87–115)	110 (104–123)	87 (82–97)	<.001
Platelet count ($\times 10^9$/L) (*n* = 36)	292 (194–342)	294 (146–324)	284 (205–408)	.65
C-reactive protein level (mg/L) (*n* = 32)	58.5 (22.8–155)	73 (18–172)	44 (23–139)	.85
Ferritin level (μg/L) (*n* = 24)	1289 (777–2124)	1364 (618–1957)	1289 (973–3941)	.26
Alanine aminotransferase level (IU/L) (*n* = 34)	75 (42–119)	70 (45–102)	89 (31–123)	.55
Aspartate aminotransferase level (U/L) (*n* = 34)	48 (33–69)	55 (34–68)	40 (30–72)	.49
Urea level (mmol/L) (*n* = 35)	13 (6.5–22)	7 (5.5–12)	18 (12–28)	.026
Creatinine level (μmol/L) (*n* = 35)	112 (62–221)	68 (59–101)	165 (100–247)	.09
Prothrombin time (sec) (*n* = 30)	14 (13–15)	14 (13–15)	14 (13–15)	.5
Fibrinogen (g/L) (*n* = 32)	6.9 (5.5–8.4)	8.2 (7–9.3)	6.4 (5.2–8)	.06
D-dimer level (mg/L) (*n* = 28)	2.9 (1.5–3.9)	1.7 (0.7–3.5)	3.4 (2.3–4)	.08
Immunologic tests data are *n/N* (%)				
Lupus anticoagulant (*n* = 19)	15/19 (79)	5/6 (83)	10/13 (77)	<.99
Other antiphospholipid antibody (*n* = 8)	4/8 (50)	2/3 (67)	2/5 (40)	<.99
Antinuclear antibody (*n* = 11)	5/11 (46)	1/2 (50)	4/9 (44)	<.99

Note.—Unless otherwise indicated, data are medians and data in parentheses are the interquartile range. *N* is the total number of patients with available data, and *n* is the number of patients with positive findings. $P < .05$ indicates a significant difference.

* Data are numbers of patients, and data in parentheses are percentages.

Table 3: Cerebrospinal Fluid Analysis

CSF Analysis	All Patients	Nonhemorrhagic Forms	Hemorrhagic Forms	*P* Values
Markers of inflammation (*n* = 31)	21/31 (68)	10/16 (63)	11/15 (73)	.7
High white blood cell count (*n* = 31)	14/31 (45)	8/16 (50)	6/15 (40)	.72
Low glycorrhachia (*n* = 31)	0	…	…	…
High proteinorachia (*n* = 31)	11/31 (36)	6/16 (38)	5/15 (33)	<.99
Elevated IgG level (*n* = 16)	7/16 (44)	3/6 (50)	4/10 (40)	<.99
Presence of oligoclonal IgG bands with the same pattern in serum (*n* = 13)	6/13 (46)	1/4 (25)	5/9 (56)	.55
Positive RT-PCR SARS-CoV-2 (*n* = 28)	1/28 (4)	1/14 (7)	0/14 (0)	<.99
High interleukin-6 level (*n* = 6)	2/6 (33)	0/1 (0)	2/5 (40)	<.99
High interleukin-10 level (*n* = 6)	1/6 (17)	1/1 (100)	0/5 (0)	.16

Note.—Unless otherwise indicated, data are numbers of patients and data in parentheses are percentages. *N* is the total number of patients with available data, and *n* is the number of patients with positive findings. CSF = cerebrospinal fluid, IgG = immunoglobulin G, IQR = interquartile range, RT-PCR = reverse transcriptase polymerase chain reaction, SARS-CoV-2 = severe acute respiratory syndrome coronavirus disease 2.

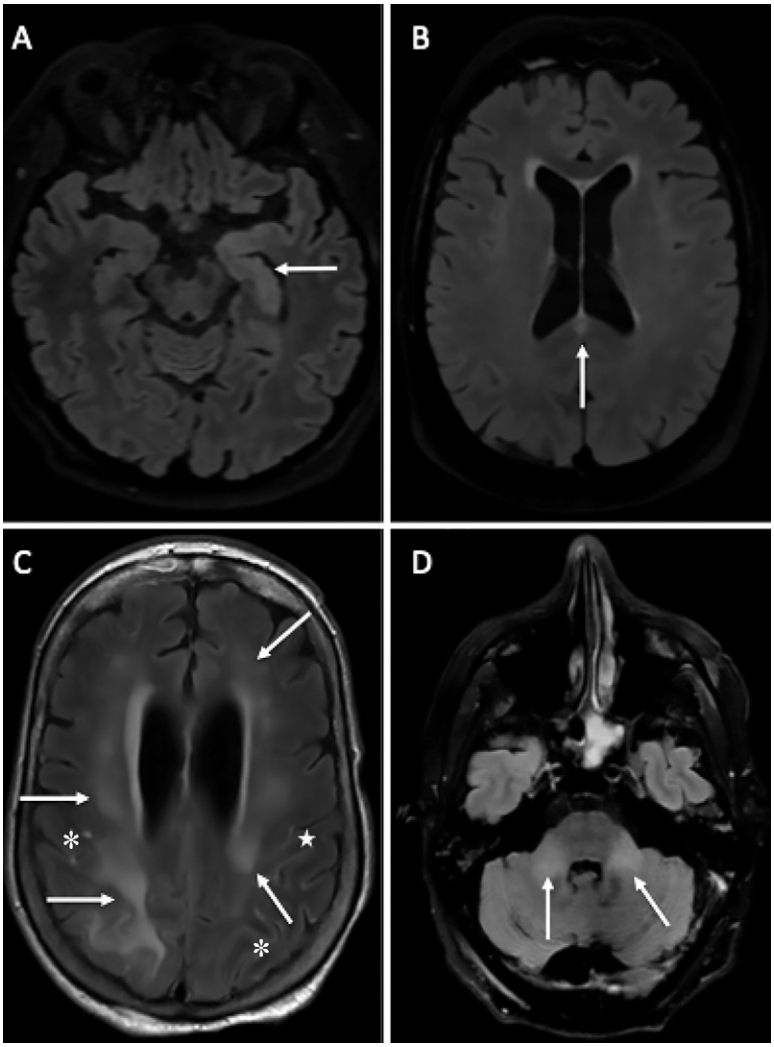

Figure 2: Axial fluid-attenuated inversion recovery (FLAIR) images in four different patients with coronavirus disease 2019. *A*, A 58-year-old man with impaired consciousness has FLAIR hyperintensities (arrow) in the left medial temporal lobe. *B*, A 66-year-old man with impaired consciousness has a FLAIR ovoid hyperintense lesion (arrow) in the central part of the splenium of the corpus callosum. *C*, A 71-year-old woman with abnormal wakefulness after sedation has extensive and confluent supratentorial white matter FLAIR hyperintensities (arrows) in association with leptomeningeal enhancement (*). *D*, A 61-year-old man with confusion has hyperintense lesions (arrows) involving both middle cerebellar peduncles.

microhemorrhages. The presence of hemorrhage was frequent, and its detection is of clinical importance, as it was associated with worse respiratory, neurologic, and biologic status. Nevertheless, the underlying mechanism of brain abnormalities remains unsolved, and the direct implication of severe acute respiratory syndrome coronavirus 2 (SARS-CoV-2) is not clear, as only one patient had positive findings for SARS-CoV-2 RNA in the cerebrospinal fluid.

Unilateral FLAIR or diffusion-weighted hyperintensities in the medial temporal lobe were frequent and have been previously reported in one patient with COVID-19 (10). The latter is frequently observed in case of infectious encephalitis (especially with some viruses like herpes simplex virus, human herpesvirus 6, or Epstein-Barr virus) or in association with autoimmune limbic encephalitis (19).

Nonconfluent multifocal WM hyperintense lesions on FLAIR and diffusion-weighted images with variable enhancement, which could be associated with hemorrhagic lesions, have rarely been reported in patients with COVID-19 (20). The latter presentation is close to what can be observed on brain MRI scans in case of an inflammatory demyelinating disease, such as acute disseminated encephalomyelitis or acute hemorrhagic leukoencephalitis. However, these latter two diagnoses cannot only be retained on the radiologic presentation without the typical cerebrospinal fluid analysis or clinical presentation (21,22). Several putative mechanisms underlying neurologic consequences of COVID-19 are evoked, and among them are immunologic parainfectious processes (23). The immunologic assumption is also reinforced by a recent neuropathologic study, which described acute disseminated encephalomyelitislike lesions in the subcortical WM in a patient with severe COVID-19 (24).

Extensive and isolated WM microhemorrhages pattern was recently described in seven critically

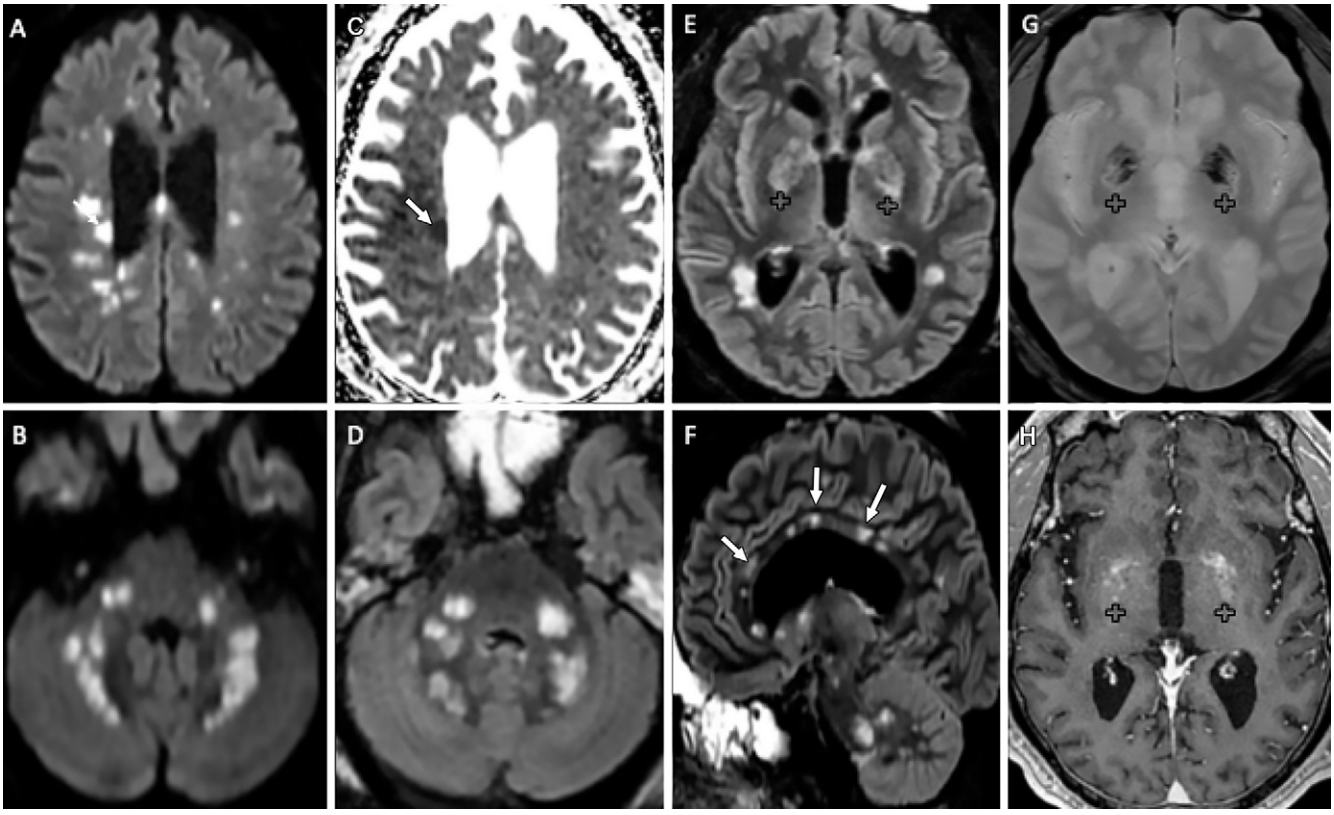

Figure 3: Images in a 65-year-old man with abnormal wakefulness after sedation. Nonconfluent multifocal white matter hyperintense lesions on fluid-attenuated inversion recovery (FLAIR) and diffusion, with variable enhancement, and hemorrhagic lesions. *A*, *B*, Axial diffusion-weighted images; *C*, apparent diffusion coefficient (ADC) map; *D*, *E*, axial FLAIR images; *F*, sagittal FLAIR image; *G*, axial susceptibility-weighted image; and *H*, contrast-enhanced T1-weighted MRI scan. Multiple nodular hyperintense diffusion and FLAIR lesions localized in the white matter including the, *F*, corpus callosum. Some (arrows) are associated with reduced ADC corresponding to *C*, cytotoxic edema. *E*, *G*, *H*, Other lesions are located next to the lenticular nucleus (+), with, *G*, hemorrhagic changes, and enhancement after contrast material administration.

ill patients with COVID-19 (12) and in the neuropathology study mentioned earlier (24). A similar pattern was recently described in one case (25) with disseminated intravascular coagulation. However, according to the criteria endorsed by the International Society on Thrombosis and Haemostasis (27), when they were available, no case of disseminated intravascular coagulation was present in our cohort. Its precise pathophysiology remains uncertain and will require further studies. Radmanesh et al (12) evoked the assumptions of hypoxia or small-vessel vasculitis.

A few patients had extensive and confluent supratentorial WM FLAIR hyperintensities (Fig 2), as previously described by Kandemirli et al (11) and Radmanesh et al (12). Its precise pathophysiology remains unclear; viral encephalitis (not supported by cerebrospinal fluid analysis) or postinfectious demyelinating diseases, as previously mentioned, may be evoked. Because most of these patients were admitted to intensive care units for acute respiratory distress syndrome, more general assumptions may be considered, such as delayed posthypoxic leukoencephalopathy (27), metabolic or toxic encephalopathy, and posterior reversible encephalopathy syndrome. This last hypothesis is in accordance with recently published nonhemorrhagic and hemorrhagic posterior reversible encephalopathy syndrome in patients with COVID-19 (28).

Even if this national neuroimaging cohort remains unique, our study has several limitations, mainly due to its retrospective design. The main limitation is that certain laboratory data were missing for some patients, notably the immunologic tests. Moreover, patients' outcomes were not always known at the time of this writing. Thus, the mortality rate is probably underestimated in our cohort.

In conclusion, in this multi-institutional study, we report 37 patients with coronavirus disease 2019 and abnormal brain MRI scans (excluding ischemic infarcts). Three main neuroradiologic patterns could be distinguished, and the presence of hemorrhage was associated with worse clinical status. Severe acute respiratory syndrome coronavirus 2 RNA was detected in the cerebrospinal fluid in only one patient, and the underlying mechanisms of brain involvement remain unclear. Imaging and neurologic follow-up must be undertaken to evaluate the prognosis of these patients.

Complete list of authors (listed alphabetically except for first and last author): Stéphane Kremer, MD, PhD; Gilles Adam, MD; Manel Alleg, MD; Mathieu Anheim, MD, PhD; René Anxionnat, MD, PhD; François-Daniel Ardellier, MD; Seyyid Baloglu, MD; Blanche Bapst, MD; Joseph Benzakoun, MD; Jérome Berge, MD; Federico Bolognini, MD; Fabrice Bonneville, MD, PhD; Grégoire Bornet, MD; Clotilde Boulay, MD; Grégoire Boulouis, MD; Claire Boutet, MD, PhD; Jean Christophe Brisset, PhD; Sophie Caillard, MD, PhD; Sophie Carré, MD; Béatrice Carsin-Nicol, MD; Olivier Collange, MD, PhD; Pierre-Olivier Comby, MD; Jean

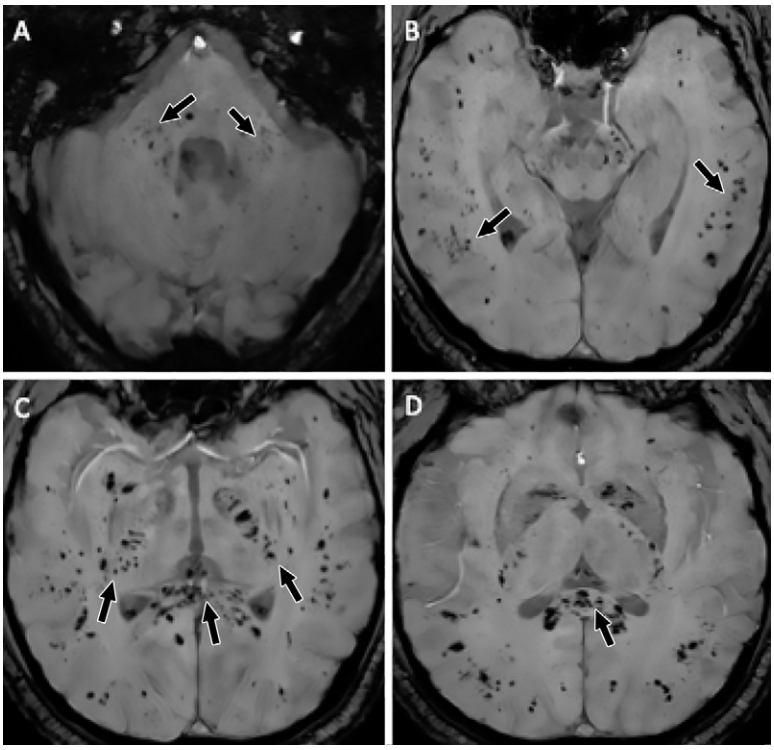

Figure 4: Axial susceptibility-weighted images in a 57-year-old man with abnormal wakefulness after sedation show extensive and isolated white matter microhemorrhages mainly affecting the, *A*, cerebellar peduncles, *B*, subcortical white matter, *C*, internal capsule, and, *D*, corpus callosum.

Marc Constans, MD, PhD; Jean-Stéphane David, MD, PhD; Isaure de Beaurepaire, MD; Jérome de Sèze, MD, PhD; Louis Delamarre, MD; Hubert Desal, MD, PhD; Myriam Edjlali-Goujon, MD, PhD; Xavier Fabre, MD; Samira Fafi-Kremer, PharmD, PhD; Jean-Christophe Ferré, MD, PhD; Philippe Feuerstein, MD; Marie-Cécile Henry Feugeas, MD, PhD; Géraud Forestier, MD; Augustin Gaudemer, MD; Thomas Geeraerts, MD, PhD; Sylvie Grand, MD; Yves Hansmann, MD, PhD; Adrien Heintz, PhD; Julie Helms, MD, PhD; Céline Hemmert, MD; Ghazi Hmeydia, MD; Lavinia Jager, MD; Apolline Kazémi, MD; Basile Kerleroux, MD; Antoine Khalil, MD; Alexandre Krainik, MD, PhD; Audrey Lacalm, MD; Augustin Lecler, MD, PhD; Claire Lecocq, MD; Nicolas Lefèbvre, MD; François Lersy, MD; Adel Maamar, MD; Guillaume Martin-Blondel, MD, PhD; Muriel Matthieu, PhD; Imen Megdiche, MD; Paul-Michel Mertes, MD, PhD; Julien Messié, MD; Serge Metanbou, MD; Nicolas Meyer, MD, PhD; Ferhat Meziani, MD; Véronique Mutschler, MD; Patrick Nesser, MD; Hélène Oesterlé, MD; Mickael Ohana, MD, PhD; Catherine Oppenheim, MD, PhD; Nadya Pyatigorskaya, MD, PhD; Marie Rafiq, MD; Frédéric Ricolfi, MD, PhD; Suzana Saleme, MD; Maleka Schenck, MD; Emmanuelle Schmitt, MD; Francis Schneider, MD, PhD; Nathan Sebag, MD; Yannick Talla Mba, MD; Pierre Thouant, MD; Thibault Willaume, MD; François Zhu, MD; Pierre-Emmanuel Zorn, PhD; François Cotton, MD, PhD.

Author affiliations: Hôpitaux Universitaires de Strasbourg, Service d'Imagerie 2, Hôpital de Hautepierre, Strasbourg, France (S.K., F.L., S.B., F.D.A., T.W.); Engineering Science, Computer Science and Imaging Laboratory (ICube), Integrative Multimodal Imaging in Healthcare, UMR 7357, University of Strasbourg-CNRS, Strasbourg, France (S.K.); Service de Neurologie, Hôpitaux Universitaires de Strasbourg, Strasbourg, France (J.d.S., C. Boulay, V.M., M. Anheim); CHU Rennes, Department of Neuroradiology, Rennes, France (J.C.F., B.C.N.); Service de Maladies Infectieuses et Réanimation Médicale, CHU Rennes, France (A.M.); Hôpitaux Universitaires de Strasbourg, Service d'Anesthésie-Réanimation, Nouvel Hôpital Civil, Strasbourg, France (O.C., P.M.M.); Service de Neuroradiologie, CHU Toulouse, Toulouse, France (F. Bonneville., G.A.); Department of Infectious and Tropical Diseases, Toulouse University Hospital, Toulouse, France (G.M.B.); Department of Neurology, Toulouse University Hospital, Toulouse, France (M.R.); Department of Anesthesia and Critical Care, Toulouse University Hospital University Toulouse 3-Paul Sabatier, Toulouse, France (T.G., L.D.); Service de Neuroradiologie Diagnostique et Interventionnelle, Centre Hospitalier Universitaire des Alpes, Grenoble, France (S.G., A. Krainik); Nephrology and Transplantation Department, Hôpitaux Universitaires de Strasbourg, Inserm UMR S1109, LabEx Transplantex, Fédération de Médecine Translationnelle de Strasbourg (FMTS), Université de Strasbourg, Strasbourg, France (S. Caillard); EA CHIMERE 7516, Université de Picardie Jules Verne, Amiens, France; Service de NeuroRadiologie, Pôle Imagerie Médicale, Centre Hospitalo-Universitaire d'Amiens, Amiens, France (J.M.C., A.H.); Service de Neuro Radiologie, Pôle Imagerie Médicale, Centre Hospitalo-Universitaire d'Amiens, Amiens, France (S.M.); Hôpitaux Universitaires de Strasbourg, Service de Médecine Intensive Réanimation, Nouvel Hôpital Civil, Strasbourg, France (J.H., F.M.); Immuno-Rhumatologie Moléculaire, INSERM UMR_S1109, LabEx TRANSPLANTEX, Centre de Recherche d'Immunologie et d'Hématologie, Faculté de Médecine, Fédération Hospitalo-Universitaire (FHU) OMICARE, Fédération de Médecine Translationnelle de Strasbourg (FMTS), Université de Strasbourg (UNISTRA), Strasbourg, France (J.H.); Hôpitaux Universitaires de Strasbourg, Service de Médecine Intensive Réanimation, Hautepierre, Strasbourg, France (M.S., F.S.); Service de Maladies Infectieuses, NHC, CHU de Strasbourg, Strasbourg, France (N.L., Y.H.); Service de Radiologie, CHU de Saint-Etienne, Saint-Etienne, France (C. Boutet); Service de Réanimation, CH de Roanne, Roanne, France (X.F.); University Hospital of Limoges, Neuroradiology Department, Limoges, France (G.F., S.S.); Radiology Department, Hôpital Privé d'Antony, Antony, France (I.d.B., G. Bornet); Service d'Imagerie Pédiatrique et Fœtale, Hôpital Femme Mère Enfant, HCL, Lyon, France (A. Lacalm); Service de Neuroradiologie, Hôpitaux Civils de Colmar, Colmar, France (H.O., F. Bolognini, J.M.); INSERM U1266, Service d'Imagerie Morphologique et Fonctionnelle, GHU Psychiatrie et Neurosciences, Site Sainte-Anne, Paris, France (G.H., J. Benzakoun, C.O., G. Boulouis, M.E.G., B.K.); Service de Neuroradiologie, CHU Henri Mondor, Créteil, France (B.B., I.M.); Neuroradiology Unit, Department of Radiology, Assistance Publique–Hôpitaux de Paris (APHP), Bichat University Hospital, Paris, France (M.C.H.F., A.G.); Department of Radiology, Assistance Publique–Hôpitaux de Paris (APHP), Denis Diderot University and Medical School, Bichat University Hospital, Paris, France (A. Khalil); CHIC Unisanté, Hôpital Marie Madeleine, Forbach, France (L.J., P.N., Y.T.M.); Service de Radiologie 1, GHR Mulhouse Sud Alsace, Hôpital Mère Enfants, Mulhouse, France (C.H., P.F., N.S.); Service de Neurologie, Centre Hospitalier de Haguenau, Haguenau, France (S. Carré, C.L.); Service de Radiologie, Centre Hospitalier de Haguenau, Haguenau, France (M. Alleg); Service de Neuroradiologie, Hôpital Central, CHU de Nancy, Nancy, France (E.S., R.A., F.Z.); Department of Neuroradiology, University Hospital of Dijon, Hôpital François Mitterrand, Dijon, France (P.O.C., F.R., P.T.); Department of Diagnostic and Interventional Neuroradiology, University Hospital, Nantes, France (H.D.); Neuroradiology Department, CHU de Bordeaux, Bordeaux, France (J. Berge); Service de Neuroradiologie, CHU de Lille, Lille, France (A. Kazémi); Assistance Publique Hôpitaux de Paris, Service de Neuroradiologie, Hôpital Pitié-Salpêtrière, Paris, France Sorbonne Université, Univ Paris 06, UMR S 1127, CNRS UMR 7225, ICM, F-75013, Paris, France (N.P.); Neuroradiology Department, Fondation A. Rothschild Hospital, Paris, France (A. Lecler); Hôpitaux Universitaires de Strasbourg, UCIEC, Pôle d'Imagerie, Strasbourg, France (P.E.Z., M.M.); Observatoire Français de la Sclérose en Plaques, Lyon, France (J.C.B.); Hôpitaux Universitaires de Strasbourg, Laboratoire de Virologie Médicale, Strasbourg, France (S.F.K.); Radiology Department, Nouvel Hôpital Civil, Strasbourg University Hospital, Strasbourg, France (M.O.); INSERM (French National Institute of Health and Medical Research), UMR 1260, Regenerative Nanomedicine (RNM), FMTS, Strasbourg, France (F.M.); Department of Anaesthesia and Intensive Care, Lyon-Sud Hospital, Hospices Civils de Lyon, F-69495 Pierre Benite; University Claude Bernard Lyon 1, Lyon, France (J.S.D.); CHU de Strasbourg, Service de Santé Publique, GMRC, F-67091 Strasbourg, France (N.M.); Institut de Génétique et de Biologie Moléculaire et Cellulaire (IGBMC), INSERM-U964/CNRS-UMR7104/Université de Strasbourg, Illkirch, France (M. Anheim); MRI Center, Centre Hospitalier Lyon Sud, Hospices Civils de Lyon, Lyon, France (F.C.); and Université Lyon 1, CREATIS-LRMN, CNRS/UMR/5220-INSERM U630, Villeurbanne, France (F.C.).

Author contributions: Guarantors of integrity of entire study: S.K., F.L., J.d.S., B.C.N., F. Bonneville, G.A., M.S., B.B., C.H., S. Carré, P.O.C., P.T., S.S., B.K., M.M., S.B., Y.H., P.M.M., F.S., F.C. Study concepts/study design or data acquisition or data analysis/interpretation: all authors; manuscript drafting or manuscript revision for important intellectual content: all authors; approval of final version of submitted manuscript: all authors; agrees to ensure any questions related to the work are appropriately resolved: all authors; literature research: S.K., F.L., B.C.N., F. Bonneville, T.G., J.M.C., J.H., M.S., G. Bornet, A. Lacalm, H.O., F. Bolognini, J.M., M.C.H.F., A. Khalil, L.J., P.F., S. Carré,

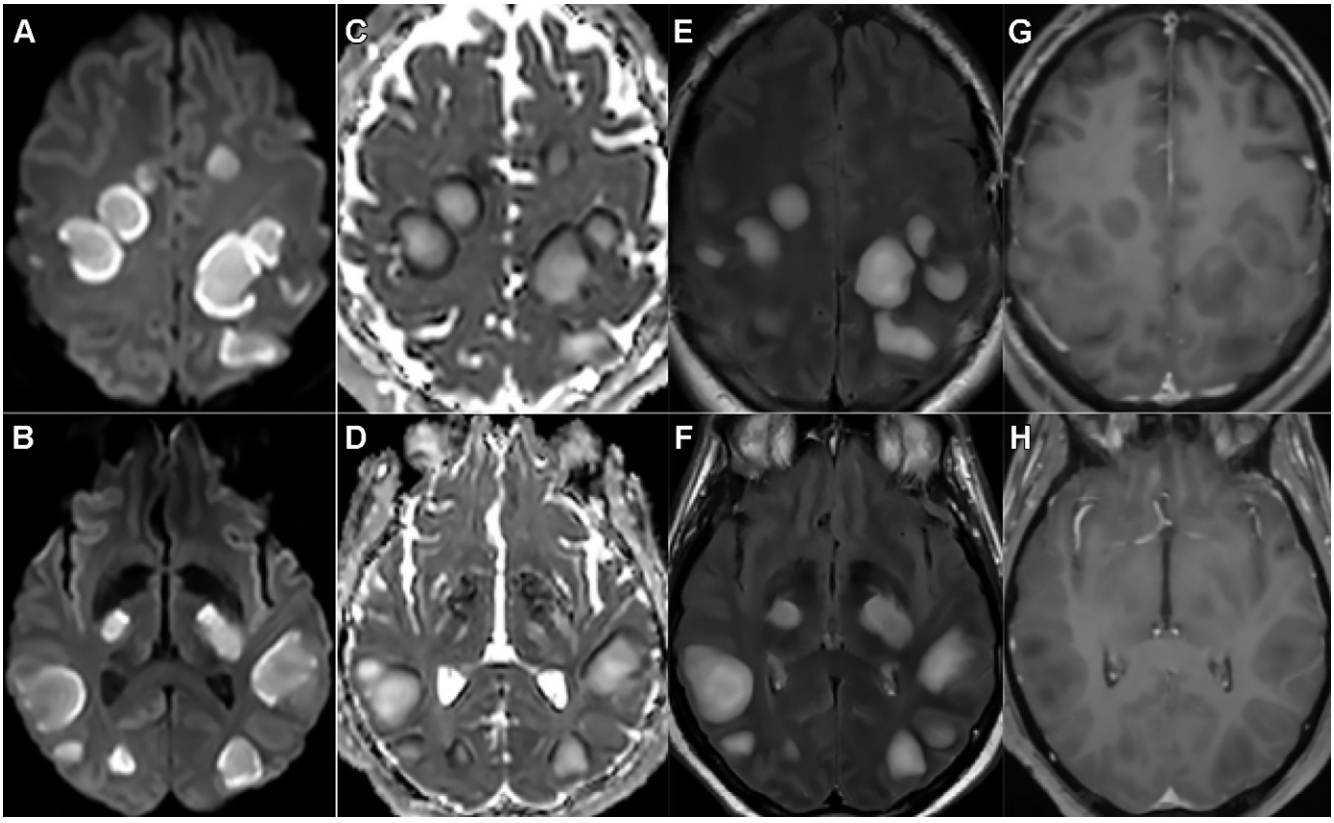

Figure 5: Images in a 54-year-old man with abnormal wakefulness after sedation. Nonconfluent multifocal white matter hyperintense lesions on fluid-attenuated inversion recovery (FLAIR) and diffusion-weighted images, with variable enhancement. *A*, *B*, Axial diffusion, *C*, *D*, apparent diffusion coefficient (ADC) map, *E*, *F*, axial contrast-enahnced FLAIR, and, *G*, *H*, contrast-enhanced T1-weighted MRI scans. Multiple nodular hyperintense diffusion and FLAIR subcortical and corticospinal tracts lesions, with very mild mass effect on adjacent structures. *C*, *D*, The lesions present a center with an elevation of ADC corresponding to vasogenic edema and a peripheral ring of reduced ADC corresponding to cytotoxic edema. After contrast material administration, *G*, *H*, small areas of very mild enhancement are detected.

C.L., E.S., F.R., A. Lecler, M.E.G., S.B., T.W., J.C.B., F.S., M. Anheim, F.C.; clinical studies: S.K., J.d.S., J.C.F., A.M., B.C.N., O.C., F. Bonneville, G.A., G.M.B., M.R., T.G., L.D., S.G., A. Krainik, S. Caillard, J.M.C., S.M., A.H., J.H., M.S., N.L., C. Boutet, X.F., I.d.B., G. Bornet, A. Lacalm, H.O., F. Bolognini, G.H., J. Benzakoun, C.O., B.B., I.M., M.C.H.F., A.G., L.J., P.N., Y.T.M., P.F., N.S., S. Carré, C.L., E.S., R.A., F.Z., P.O.C., F.R., P.T., H.D., J. Berge, A. Kazémi, N.P., A. Lecler, S.S., B.K., M.M., S.B., C. Boulay, V.M., Y.H., F.S., M.O., F.M., M. Anheim, F.C.; experimental studies: F.L., J.C.F., B.C.N., J.M.C., G. Bornet, A. Lacalm, H.O., M.C.H.F., A. Khalil, L.J., C.H., N.S., E.S., F.R., J. Berge, A. Lecler; statistical analysis: F.L., B.C.N., J.M.C., G. Bornet, A. Lacalm, M.C.H.F., L.J., E.S., F.R., P.E.Z., N.M.; and manuscript editing: S.K., F.L., J.d.S., J.C.F., B.C.N., F. Bonneville, G.M.B., T.G., J.M.C., J.H., N.L., C. Boutet, G. Bornet, A. Lacalm, J. Benzakoun, C.O., B.B., M.C.H.F., A.G., L.J., C.L., E.S., F.R., G. Boulouis, J. Berge, N.P., A. Lecler, M.E.G., B.K., S.B., T.W., J.C.B., P.M.M., F.S., S.F.K., M.O., J.S.D., N.M., M. Anheim, F.C.

Author contributions: Guarantors of integrity of entire study, S.K., F.L., J.d.S., B.C.N., F. Bonneville, G.A., M.S., B.B., C.H., S. Carré, P.O.C., P.T., S.S., B.K., M.M., S.B., Y.H., P.M.M., F.S., F.C. The complete list of author contributions is at the end of this article. Conflicts of interest are listed at the end of this article.

Disclosures of Conflicts of Interest: S.K. disclosed no relevant relationships. **G.A.** disclosed no relevant relationships. **M. Alleg** disclosed no relevant relationships. **M. Anheim** Activities related to the present article: disclosed no relevant relationships. Activities not related to the present article: is on the board of AbbVie and Orkyn; received grants from Actelion Pharmaceuticals and Johnson & Johnson; gave lectures for AbbVie, Actelion Pharmaceuticals, Teva, LVL, Merz, and Aguettant; developed educational presentations for Actelion Pharmaceuticals, Aguettant, Merz, LVL, and Teva; was compensated for travel by AbbVie, LVL, Actelion Pharmaceuticals, Aguettant, and Merz. Other relationships: disclosed no relevant relationships. **R.A.** disclosed no relevant relationships. **F.D.A.** disclosed no relevant relationships. **S.B.** disclosed no relevant relationships. **B.B.** disclosed no relevant relationships. **J. Benzakoun** disclosed no relevant relationships. **J. Berge** disclosed no relevant relationships. **F. Bolognini** disclosed no relevant relationships. **F. Bonneville** disclosed no relevant relationships. **G. Bornet** disclosed no relevant relationships. **C. Boulay** disclosed no relevant relationships. **G. Boulouis** disclosed no relevant relationships. **C. Boutet** disclosed no relevant relationships. **J.C.B.** Activities related to the present article: disclosed no relevant relationships. Activities not related to the present article: is employed by Median Technologies. Other relationships: disclosed no relevant relationships. **S. Caillard** disclosed no relevant relationships. **S. Carré** disclosed no relevant relationships. **B.C.** disclosed no relevant relationships. **O.C.** Activities related to the present article: disclosed no relevant relationships. Activities not related to the present article: is on the board of Edwards Lifesciences, gave lectures for Smiths Medical France, was compensated for travel by Pfizer. Other relationships: disclosed no relevant relationships. **P.O.C.** disclosed no relevant relationships. **J.M.C.** disclosed no relevant relationships. **J.S.D.** disclosed no relevant relationships. **I.d.B.** disclosed no relevant relationships. **J.D.S.** disclosed no relevant relationships. **L.D.** disclosed no relevant relationships. **H.D.** disclosed no relevant relationships. **M.E.** disclosed no relevant relationships. **X.F.** disclosed no relevant relationships. **S.F.** disclosed no relevant relationships. **J.C.F.** disclosed no relevant relationships. **P.F.** disclosed no relevant relationships. **M.C.H.F.** disclosed no relevant relationships. **G.F.** disclosed no relevant relationships. **A.G.** disclosed no relevant relationships. **T.G.** disclosed no relevant relationships. **S.G.** disclosed no relevant relationships. **Y.H.** Activities related to the present article: disclosed no relevant relationships. Activities not related to the present article: gave lectures for Pfizer, Sanofi, and Gilead, Janssen, and Astellas. Other relationships: disclosed no relevant relationships. **A.H.** disclosed no relevant relationships. **J.H.** disclosed no relevant relationships. **C.H.** disclosed no relevant relationships. **G.H.** disclosed no relevant relationships. **L.J.** disclosed no relevant relationships. **A. Kazémi** disclosed no relevant relationships. **B.K.** disclosed no relevant relationships. **A. Khalil** disclosed no relevant relationships. **A. Krainik** disclosed no relevant relationships. **A. Lacalm** disclosed no relevant relationships. **A. Lecler** disclosed no relevant relationships. **C.L.** disclosed no relevant relationships. **N.L.** disclosed no relevant relationships. **F.L.** disclosed no relevant relationships. **A.M.** disclosed no relevant relationships. **G.M.** disclosed no relevant relationships. **M.M.** disclosed no relevant relationships. **I.M.** disclosed no

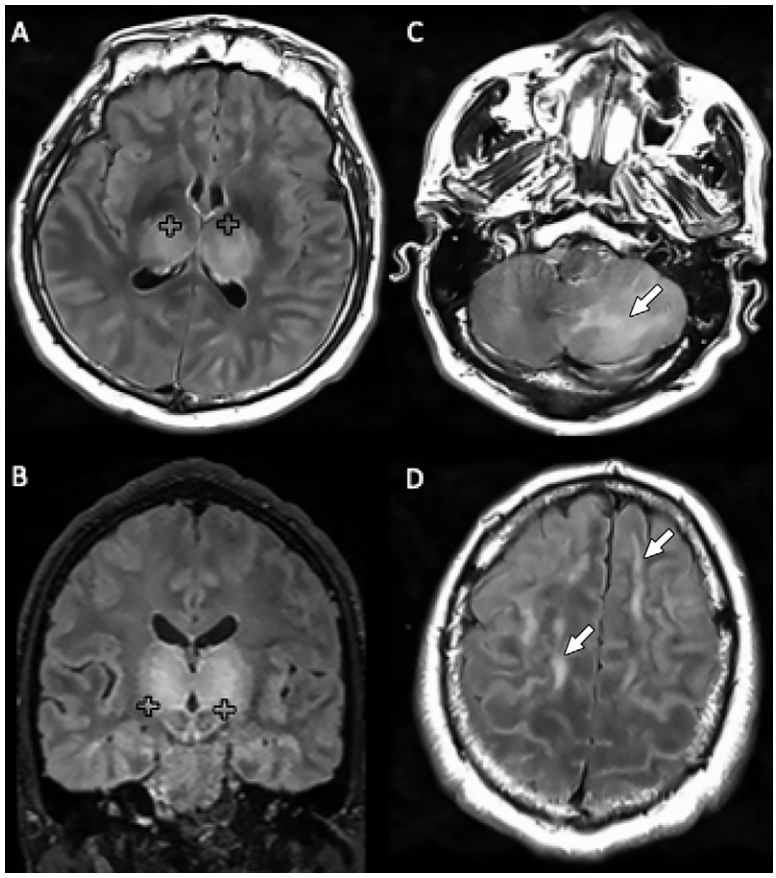

Figure 6: Images in a 51-year-old man with impaired consciousness and acute necrotizing encephalopathy. *A*, *C*, *D*, Axial fluid-attenuated inversion recovery (FLAIR), and, *B*, coronal FLAIR images show bilateral FLAIR hyperintensity (+) in, *A*, *B*, both thalami associated with involvement of the, *C*, cerebellar, and, *D*, cerebral white matter (arrows).

relevant relationships. **P.M.** disclosed no relevant relationships. **J.M.** disclosed no relevant relationships. **S.M.** disclosed no relevant relationships. **N.M.** disclosed no relevant relationships. **F.M.** disclosed no relevant relationships. **V.M.** disclosed no relevant relationships. **P.N.** disclosed no relevant relationships. **H.O.** disclosed no relevant relationships. **M.O.** Activities related to the present article: disclosed no relevant relationships. Activities not related to the present article: is a consultant for Canon Medical Systems Europe. Other relationships: disclosed no relevant relationships. **C.O.** disclosed no relevant relationships. **N.P.** Activities related to the present article: disclosed no relevant relationships. Activities not related to the present article: gave lectures for GE Healthcare and Biogen. Other relationships: disclosed no relevant relationships. **M.R.** disclosed no relevant relationships. **F.R.** disclosed no relevant relationships. **S.S.** disclosed no relevant relationships. **M.S.** disclosed no relevant relationships. **E.S.** disclosed no relevant relationships. **F.S.** disclosed no relevant relationships. **N.S.** disclosed no relevant relationships. **Y.T.M.** disclosed no relevant relationships. **P.T.** disclosed no relevant relationships. **T.W.** disclosed no relevant relationships. **F.Z.** disclosed no relevant relationships. **P.E.** disclosed no relevant relationships. **F.C.** disclosed no relevant relationships.

References

1. Zhu N, Zhang D, Wang W, et al. A novel coronavirus from patients with pneumonia in China, 2019. N Engl J Med 2020;382(8):727–733.
2. Bohmwald K, Gálvez NMS, Ríos M, Kalergis AM. Neurologic alterations due to respiratory virus infections. Front Cell Neurosci 2018;12:386.
3. Desforges M, Le Coupanec A, Stodola JK, Meessen-Pinard M, Talbot PJ. Human coronaviruses: viral and cellular factors involved in neuroinvasiveness and neuropathogenesis. Virus Res 2014;194:145–158.
4. Desforges M, Le Coupanec A, Dubeau P, et al. Human coronaviruses and other respiratory viruses: underestimated opportunistic pathogens of the central nervous system? Viruses 2019;12(1):E14.
5. Li Y, Li H, Fan R, et al. Coronavirus infections in the central nervous system and respiratory tract show distinct features in hospitalized children. Intervirology 2016;59(3):163–169.
6. Arabi YM, Harthi A, Hussein J, et al. Severe neurologic syndrome associated with Middle East respiratory syndrome corona virus (MERS-CoV). Infection 2015;43(4):495–501.
7. Kim JE, Heo JH, Kim HO, et al. Neurological complications during treatment of Middle East respiratory syndrome. J Clin Neurol 2017;13(3):227–233.
8. Yeh EA, Collins A, Cohen ME, Duffner PK, Faden H. Detection of coronavirus in the central nervous system of a child with acute disseminated encephalomyelitis. Pediatrics 2004;113(1 Pt 1):e73–e76.
9. Poyiadji N, Shahin G, Noujaim D, Stone M, Patel S, Griffith B. COVID-19-associated acute hemorrhagic necrotizing encephalopathy: CT and MRI Features. Radiology 2020. 10.1148/radiol.2020201187. Published online March 31, 2020.
10. Moriguchi T, Harii N, Goto J, et al. A first case of meningitis/encephalitis associated with SARS-Coronavirus-2. Int J Infect Dis 2020;94:55–58.
11. Kandemirli SG, Dogan L, Sarikaya ZT, et al. Brain MRI findings in patients in the intensive care unit with COVID-19 infection. Radiology doi:10.1148/radiol.2020201697. Published online May 8, 2020.
12. Radmanesh A, Derman A, Lui YW, et al. COVID-19 -associated diffuse leukoencephalopathy and microhemorrhages. Radiology doi:10.1148/radiol.2020202040. Published online May 21, 2020.
13. Franceschi AM, Ahmed O, Giliberto L, Castillo M. Hemorrhagic posterior reversible encephalopathy syndrome as a manifestation of COVID-19 infection. AJNR Am J Neuroradiol 2020;41(7):1173–1176. 10.3174/ajnr.A6595. Published online May 21, 2020.
14. Mao L, Jin H, Wang M, et al. Neurologic manifestations of hospitalized patients with coronavirus disease 2019 in Wuhan, China. JAMA Neurol 2020;77(6):683–690.
15. Mahammedi A, Saba L, Vagal A, et al. Imaging in neurological disease of hospitalized COVID-19 patients: an Italian multicenter retrospective observational study. Radiology doi:10.1148/radiol.2020201933. Published online May 21, 2020.
16. Helms J, Kremer S, Merdji H, et al. Neurologic features in severe SARS-CoV-2 infection. N Engl J Med 2020;382(23):2268–2270.
17. Romero-Sánchez CM, Díaz-Maroto I, Fernández-Díaz E, et al. Neurologic manifestations in hospitalized patients with COVID-19: The ALBACOVID

registry. Neurology doi:10.1212/WNL.0000000000009937. Published online June 1, 2020.
18. World Health Organization. Protocol: Real-time RT-PCR assays for the detection of SARS-CoV-2 Institut Pasteur, Paris. https://www.who.int/docs/default-source/coronaviruse/real-time-rt-pcr-assays-for-the-detection-of-sars-cov-2-institut-pasteur-paris.pdf?sfvrsn=3662fcb6_2.
19. Budhram A, Leung A, Nicolle MW, Burneo JG. Diagnosing autoimmune limbic encephalitis. CMAJ 2019;191(19):E529–E534.
20. Parsons T, Banks S, Bae C, Gelber J, Alahmadi H, Tichauer M. COVID-19-associated acute disseminated encephalomyelitis (ADEM). J Neurol doi:10.1007/s00415-020-09951-9. Published online May 30, 2020.
21. Pohl D, Alper G, Van Haren K, et al. Acute disseminated encephalomyelitis: updates on an inflammatory CNS syndrome. Neurology 2016;87(9 Suppl 2):S38–S45.
22. Nabi S, Badshah M, Ahmed S, Nomani AZ. Weston-Hurst syndrome: a rare fulminant form of acute disseminated encephalomyelitis (ADEM). BMJ Case Rep 2016;2016:bcr2016217215.
23. Needham EJ, Chou SH, Coles AJ, Menon DK. Neurological implications of COVID-19 infections. Neurocrit Care 2020;32(3):667–671.
24. Reichard RR, Kashani KB, Boire NA, Constantopoulos E, Guo Y, Lucchinetti CF. Neuropathology of COVID-19: a spectrum of vascular and acute disseminated encephalomyelitis (ADEM)-like pathology. Acta Neuropathol (Berl) 2020;140(1):1–6.
25. Radmanesh F, Rodriguez-Pla A, Pincus MD, Burns JD. Severe cerebral involvement in adult-onset hemophagocytic lymphohistiocytosis. J Clin Neurosci 2020;76:236–237.
26. Taylor FB Jr, Toh CH, Hoots WK, Wada H, Levi M; Scientific Subcommittee on Disseminated Intravascular Coagulation (DIC) of the International Society on Thrombosis and Haemostasis (ISTH). Towards definition, clinical and laboratory criteria, and a scoring system for disseminated intravascular coagulation. Thromb Haemost 2001;86(5):1327–1330.
27. Katyal N, Narula N, George P, Nattanamai P, Newey CR, Beary JM. Delayed post-hypoxic leukoencephalopathy: a case series and review of the literature. Cureus 2018;10(4):e2481.
28. Kishfy L, Casasola M, Banankhah P, et al. Posterior reversible encephalopathy syndrome (PRES) as a neurological association in severe Covid-19. J Neurol Sci 2020;414:116943.